Regional Environmental Change (2023) 23:17
https://doi.org/10.1007/s10113-022-02016-9

ORIGINAL ARTICLE

Larch response to warming in northern Siberia

Viacheslav I. Kharuk[1,2,3] · Il'ya A. Petrov[1,2,3] · Leonid V. Krivobokov[1] · Alexey S. Golyukov[1,2,3] · Maria L. Dvinskaya[1,3] · Sergei T. Im[1,2,3,4] · Alexander S. Shushpanov[1,3,4] · Kevin T. Smith[5]

Received: 23 December 2021 / Accepted: 10 December 2022

Abstract

The dendroecology of larch (*Larix gmelinii* Rupr.) in the world's northernmost forest provided insight into the complex relationship of tree growth, forest stand establishment, and changing eco-climatic factors. The Ary-Mas forest in the northern Siberia (72° + NL) is an ecological island, surrounded by tundra. We hypothesized that the environmental constraints that limit larch growth in this harsh habitat include soil moisture and winter winds as well as low air temperature. We constructed and analyzed the larch growth index (GI) chronology from the eighteenth century until 2019. We found that the larch GI depended on the air temperature, soil moisture anomalies, and winter wind speed, and that dependence was significantly different before and after the 2000s. Larch GI responded to the onset of climatic warming in the 1970s by a minor GI increase followed by a GI decrease until the end of 1990. Increased air temperature early in the growing season favored increased GI, whereas elevated winter wind speed negatively influenced larch growth. After warming in the 2000s, the length of the growing season increased by 15 days, and larch GI was sensitive to air temperature both early and late in the growing season. The adverse influence of winter winds has gradually decreased since the 1970s, becoming a minor factor in the 2000s. Soil moisture in "wet, cold soils" negatively influenced larch growth. Meanwhile, decreased soil moisture in the northern lowlands favored increased larch growth. We found that larch growth increases were strongly correlated with GPP and NPP (gross and net primary productivity) within the Ary-Mas site and for the central Siberian Arctic. We infer that this Arctic region continues to be a carbon sink.

Keywords Larch growth · *Larix gmelinii* · Permafrost · Warming-driven growth · Wind impact · GPP · NPP · Soil moisture · Siberian Arctic

Communicated by José Valentin Roces-Diaz

✉ Il'ya A. Petrov
petrovilsoran@gmail.com

Viacheslav I. Kharuk
v7sib@mail.ru

Leonid V. Krivobokov
leo_kr@mail.ru

Alexey S. Golyukov
jedirevan@ya.ru

Maria L. Dvinskaya
mary_dvi@ksc.krasn.ru

Sergei T. Im
stim@ksc.krasn.ru

Alexander S. Shushpanov
alexandr01061987@gmail.com

Kevin T. Smith
kevin.smith3@usda.gov

[1] Sukachev Institute of Forests, Federal Scientific Center, Russian Academy of Science, Siberian Branch, Academgorodok 50/28, Krasnoyarsk 660036, Russia

[2] Siberian Federal University, Svobodny str.79, 660041 Krasnoyarsk, Russia

[3] Tomsk State University, Lenina str. 36, 634050 Tomsk, Russia

[4] Reshetnev Siberian State University of Science and Technology, Krasnoyarsky rabochy str. 31, 660014 Krasnoyarsk, Russia

[5] USDA Forest Service, 271 Mast Road, Durham, NH 03824, USA

Published online: 22 December 2022

Introduction

Forests of larch (*Larix. sibirica* Ledeb., *L. gmelinii*, and *L. cajanderi* Mayr) dominate northern Russia and the Arctic treeline and occupy 70% of the permafrost zone, primarily in open stands (Bondarev 1997; The Forest Fund of Russia 2003). Within the permafrost zone, larch outcompetes Siberian pine (*Pinus sibirica* Du Tour), spruce (*Picea obovata* Ledeb.), and Siberian fir (*Abies sibirica* Ledeb.) due to its deciduous habit and dense bark that protects against winter desiccation, snow abrasion, and fire injury. As pyrophytic species, larch are well adapted to periodic natural wildfire, due to resistance to fire injury and the ability to readily regenerate in burned areas (Abaimov et al. 2002; Kharuk et al. 2021a).

The effects of global warming have been most significant at high latitudes (Gulev et al. 2021). Since the onset of climatic warming in the 1970s, larch growth in the permafrost region has increased, accompanied by increased stand density in the northern Ural Mountains (Shiyatov et al. 2007; Esper et al. 2010) with similar patterns evident in northern Siberia (Kharuk et al. 2006; Kirdyanov et al. 2013; Wieczorek et al. 2017). Elevated air temperatures early in the growing season were considered a primary driver of increased larch growth (Kharuk et al. 2019). More generally, gross and net primary productivity (GPP and NPP, respectively) have increased in the Arctic and subarctic zones (Vickers et al. 2016; Bhatt et al. 2017; Hember et al. 2017; Kharuk et al. 2021a). Increased radial growth of larch is correlated to increased GPP estimates from remote sensing analysis (Kharuk et al. 2015, 2019). This is distinct from atmospheric warming at lower latitudes which have caused widespread conifer decline and mortality due to the combined effect of drought stress and insect attacks (e.g., Allen et al. 2015; Kharuk et al. 2017, 2021b).

During the recent decades of warming, larch has migrated into the polar and alpine tundra (Kharuk et al. 2013). Upward shifts in alpine treeline are significantly faster in subarctic than in temperate regions (Lu et al. 2021). In the Arctic permafrost zone, warming promoted the migration of less cold-resistant "southern conifers" (*Pinus sibirica*, *Abies sibirica*, and *Picea obovata*) into the larch dominance zone (Kharuk et al. 2005). Outside of the permafrost zone, climate-driven growth stimulation has been described for many boreal tree species (e.g., Kullman and Kjallgren 2006; Harsch et al. 2009; McMahon et al. 2010).

However, in recent decades, larch growth in the Siberian Arctic was less than that predicted by dendroclimatic models. The decreased growth sensitivity of larch and other conifers include a hiatus in climatic response during the 1990s and 2000s (Kharuk et al. 2019). More broadly, the deviation of recently observed growth from dendroclimatic models developed from earlier observations (the "divergence phenomenon") has been described and variously interpreted for other boreal and sub-boreal tree species (e.g., Smith et al. 1999; Andreu-Hayles et al. 2011; Lebourgeois et al. 2012). The complexity may be that although temperature has an important effect on growth, it is not the only factor that controls growth in the permafrost in the changing climate. Other variables, such as water and wind regimes, also influence vegetation growth, and their significance may be modified by ongoing changes in climate (e.g., Kullman 2005; Kirdyanov et al. 2013; Kharuk et al. 2015; Zhang et al. 2016).

In this paper, we analyze climate-driven changes in larch growth index (GI) and vegetation productivity within the Ary-Mas "forest island," the world's northernmost forest stand (72° + N). We hypothesize that in permafrost, the response of larch's to climate change may be modulated not only by warming but also by moisture and wind regimes. We seek the answer to the following questions:

How did larch growth evolve during ongoing climate change?
How has larch responded to shifts in temperature, moisture, and wind regimes in recent decades?
Does larch growth within our study site relate to broader-scale trends in GPP and NPP?

Study area

Ary-Mas in central Siberia contains the northernmost known forest stands (72°26′N/102°02′E; Fig. 1). This forest is composed of larch (*Larix gmelinii*), the frontier tree species in northern Siberia. Larch occupies terraces on the high southern bank of the Novaya River at elevations of up to 80 m a.s.l. Trees occur in strips 0.5–1.5 km wide and approximately 20 km in length along the river. Sparse stands spread away along the creeks connected to the Novaya for approximately 3–4 km. In the boggy lowland to the north, larch trees occur in wind-protected sites (e.g., around the lakes) and can be found dozens of kilometer northward.

Within Ary-Mas, larch stands are generally sparse with crown closure (CC) <0.3), although local areas may have CC >0.5. Average tree height and diameter at breast height (1.3 m above ground line, DBH) was 5–8 m and 10–14 cm, respectively with individuals reaching 10–12 m and 25 cm, respectively. Cone production begins at about 30 years of age. Cones become abundant, although the seed germination rate is low. Tree age can reach 500–700 years. Larch trees originate both from seedlings and from vegetative layering. In addition, Ary-Mas is a State reserve and a sacral forest and an important

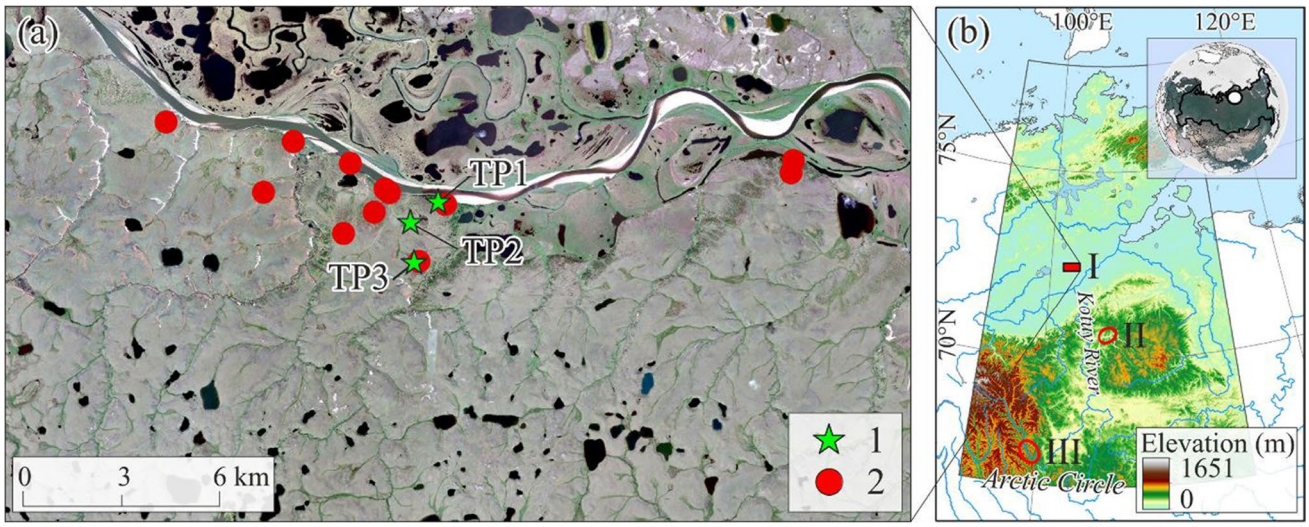

Fig. 1 **a** The Ary-Mas study area and its location within Central Siberian Arctic. Stars (1) are test plots (TP1–TP3) established in 2020. Dots (2) are TP established in 1970 and 1990. **b** Ary-Mas site (I) and supplementary sites Kotuykan (II) and Kotuy (III) (Kharuk et al. 2013, 2019)

cultural resource for indigenous people. Thus trees have rarely, if ever, been cut (Ary-Mas 1978). In addition, we compare larch at Ary-Mas to supplementary sites in Kotuy and Kotuykan (Fig. 1b) as previously described (Kharuk et al. 2013, 2019). These latter supplementary sites are typical of larch (*Larix gmelinii*) stands within the permafrost zone.

Climate

Climate of the study area is strongly continental, with an annual precipitation of 250 mm and an average air temperature of −12 °C. The relative air humidity in summer is approximately 75%. The snow cover lasts for about 245 days with maximal snow depth (30–60 cm) occurring in March. The mean July temperature is +12 °C (with maximal values up to +37 °C). The period with temperatures above the freezing point lasts approximately 110 days. However, subzero temperatures and snowfall are possible throughout the summer. The coldest months are January and February (average monthly temperature is −32 °C, absolute minimum is −59 °C). The mean winter wind speed is 4 m/s; strong winds (> 10 m/s) occurred during 40 days/year. Within the permafrost, the depth of seasonal soil thawing reaches 50–70 cm in mineralized areas, up to 1 m on steep slopes of open woodlands, and 10–30 cm under moss cover (Ary-Mas 1978).

Methods

Field studies

Field studies in Ary-Mas were conducted in July 2020. Three test plots (approximately 0.5 ha each) were established along the elevation gradient from the first terrace to the top of the watershed, a total distance of ~1 km) (Fig. 1a). Test plot 1 (TP1) was established within a closed-canopy stand (CC > 0.3). Due to tree density and age (see below), we consider TP1 to be a "larch refugium" where trees have survived despite the harsh environment. TP 2 and 3 were established in sparse stands of younger trees which we consider evidence of later recruitment due to environmental changes including warming. Tree and stand characteristics (stem diameter, tree height, stand density, regeneration, ground cover, and soil type) were determined. For dendrochronological analysis, we randomly selected trees within ~0.5 ha of the TP center. We extracted individual tree cores with an increment borer from 20 trees to represent each TP. Cores were taken at DBH height (1.3 m above ground line) from the southern-facing stem. In addition, former inventory data for twelve TPs were also used in the analysis (Norina, 1978; Annals of the State Reserve "Taimyrsky" (n.d.) http://taimyrsky.ru/letopis/letopis.htm).

Dendrochronological analysis

Increment cores (20 cores per TP; in 60 cores in total) were mounted, finely sanded, and treated with contrast powder to enhance the visualization of annual ring boundaries. Ring widths were measured on a LINTAB-6 platform with an accuracy of 0.01 mm. Ring widths were cross-dated followed by quality assessment with COFECHA software (https://www.ldeo.columbia.edu/tree-ring-laboratory/resources/software; Holmes 1983).

We found a high degree of coherence among the tree-ring measurement series from TP1-3 with the average correlation to the pooled master series as 0.68, with locally absent

rings at 1.14%. Consequently, the pooled measurement series from TP 1–3 were the basis of the dendroclimatic analysis. Since larch age difference between DBH and root levels is about 60 years (Norina 1978), we estimated tree age from ring counts plus the addition of that an age correction factor. The Ary-Mas larch chronology was developed using ARSTAN software (Cook and Holmes 1986; https://www.ldeo.columbia.edu/tree-ring-laboratory/resources/software). To reduce the effect of long-term trends unrelated to the eco-climate factors to be tested, each ring width series was fitted with a negative exponential or negative linear trend line. Then, the residual Ary-Mas chronology (RES chronology in ARSTAN) was constructed using autoregressive modeling to remove all first-order and greater autocorrelation to emphasize the high-frequency variability in radial growth associated with year-to-year changes in climate. For statistical analysis, the residual chronology was normalized by conversion to Z-scores with a mean of zero and standard deviation of 1.0 to create the larch growth index (GI). We tested the intraseasonal relationship of GI to climate variables with a moving 20-day-average window with a 5-day incremental step (Fakhrutdinova et al. 2017).

Eco-climate variables

The larch GI was analyzed against the main eco-climate variables: air temperature, precipitation, SPEI drought index (standardized precipitation-evapotranspiration index), wind speed, growth period length, and EWTA (equivalent water thickness anomalies). The latter represents total terrestrial water storage anomalies and it is characteristic of the moisture regime. The length of the seasonal growth period was defined as the number of days with $T > 0$ °C.

Air temperature, precipitation, and wind speed daily data were obtained from the nearby Khatanga station of the World Meteorological Organization (station 20,891, approximately 55 km distant from TP; 72°59′N/102°28′E). Data were obtained from the AISORI web-service (http://aisori-m.meteo.ru/waisori/).

The standardized precipitation-evapotranspiration index (SPEI) is the difference between precipitation and potential evapotranspiration and is inversely related to the degree of drought (Vicente-Serrano et al. 2010). TP1-3 were all located within the same 0.5° × 0.5° SPEI pixel (corresponding to an area of 17 × 55 km) and data were obtained from the Global Drought Monitor (http://sac.csic.es/spei). Soil moisture variation was obtained as equivalent water thickness anomalies (EWTA) as provided by NASA-JPL in GRACE data package L3 RL06 (vers. 4) for 2002–2019 from NASA-JPL (https://podaacopendap.jpl.nasa.gov/opendap/hyrax/allData/tellus/L3). TP1–3 were all located within one GRACE pixel (34 × 111 km at the study site latitude).

We calculated mean annual summer GPP (Running and Zhao 2015) and mean annual NPP (Running and Zhao 2019) values (in C, kg/ha) for the Ary-Mas site (period 2000–2020). We used 3 × 3-pixel area (i.e., 0.45 ha) for each of TP1–TP3; the central pixel coincided with the given TP. In addition, we calculated GPP and NPP temporal linear trends within the entire central Siberian Arctic for the 2000–2020 period (Figs. 1b, 9). Trends were calculated based on the Theil-Sen estimator, a non-parametric method that fits a regression line through the median of the slopes determined by all pairs of sample points (Sen 1968; Conover 1999). This estimator is less sensitive to outliers and it is more accurate than simple linear regression (Fernandes and Leblanc 2005). We obtained the Theil-Sen estimator in the Python programming language from library pymannkendall 1.4.2 (https://pypi.org/project/pymannkendall). We applied the estimator in ESRI ArcGIS software to analyze the spatial distribution of multiband raster datasets of GPP and NPP for the 2000–2020.

Statistical analysis

Four sets of statistical analysis were applied to the GI and environmental variables. Pearson correlation analysis identified significant relationships between the GI and individual climate variables. Forward-stepwise regression identified subsets of climate variables associated with variation in GI. Statistically significant regressions ($p < 0.05$) included 1–3 independent variables selected on the basis of having the lowest Akaike information criterion (AIC) (Akaike 1974). We also applied hierarchical multiple regression analysis in which an additional independent variable was added into the regression equation at each step ("block") of the analysis (Tabachnick and Fidell 2013). The hierarchical multiple regression analysis identified the contribution of each variable to variation in GI. Piecewise regression analysis was used to detect break points in time-series of larch GI, GPP, and NPP (Ryan and Porth 2007). We used StatSoft Statistica (http://statsoft.ru) and IBM SPSS Statistics Base V27 (https://www.ibm.com/analytics/spss-statistics-software) software for statistical analysis.

Results

Dynamics of eco-climatic factors

For Ary-Mas, winter temperature minima have increased since 1980 (Fig. 2a). No significant trends in precipitation were found (Fig. 2b), whereas the drought index SPEI became increasing negative since the end of the 1980s, indicating increased drought (Fig. 2c). Water storage anomalies (EWTA) became increasingly negative throughout

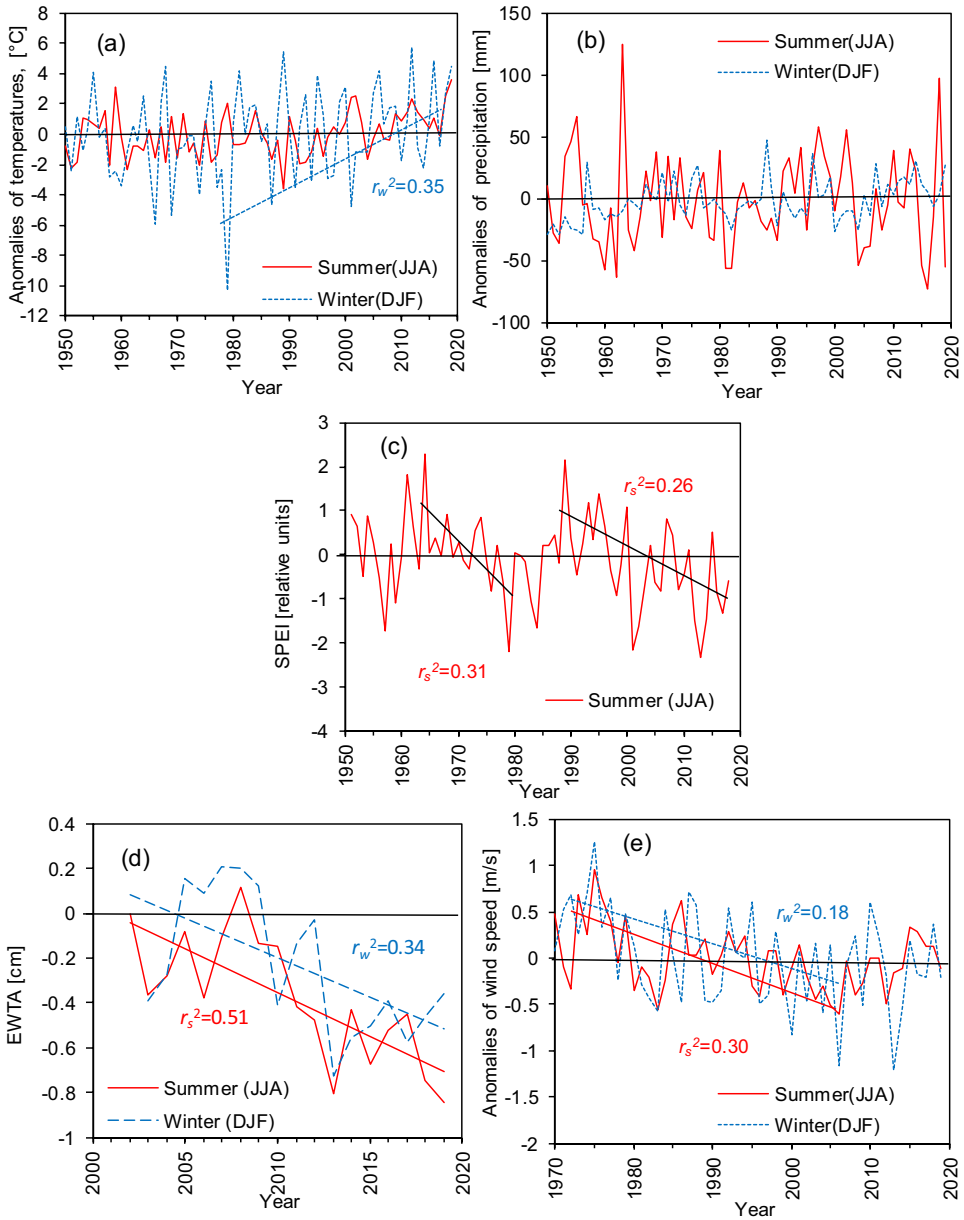

Fig. 2 Dynamics of anomalies of air temperature (**a**), precipitation (**b**), drought index SPEI (**c**), water storage (as EWTA) (**d**), and wind speed (**e**) within the Ary-Mas site. Trends are significant at $p < 0.05$

the period of available data (since 2001), which indicated decreased water storage including soil moisture content (Fig. 2d). Wind speed anomalies (both summer and winter) decreased from 1970 until about 2005 (Fig. 2e). The winter warming was accompanied by an increase in the length of the growing season, with an earlier onset of 8 days in spring and with delayed termination by 5 days in fall (Fig. 3).

Tree and test plot characteristics

Larix gmelinii was the only tree species in the three test plots, occurring on wet gley soils. Tree characteristics varied among TP1–3 including mean tree height (4.5–6.1 m), DBH (13–16 cm), and age (140–300 years at DBH height) with the regeneration density ranging from 3000–10,000 stems ha^{-1} (Table 1). Regeneration appeared generally healthy (mortality < 5%). Notably, seedling establishment mostly occurred within bare soil (e.g., within cryoturbation microsites; Fig. S1).

The shrub and herbaceous vegetation was rather similar for TP1–3. The shrub layer was composed of willow and birch (*Salix glauca* L., *S. pulchra* Cham., *Betula exilis* Sukaczev). The low shrubs and herbaceous ground cover layer contained *Ledum palustre* L., *Vaccinium vitis-idaea* L., *Carex arctisibirica* (Jurtzev) Czerep., *Cassiope tetragona* (L.) D. Don, *Eriophorum vaginatum* L., and *Equisetum arvense* L. The nearly continuous moss and lichen cover was comprised of *Dicranum acutifolium* (Lindb. &

Arnell) C.E.O.Jensen., *Aulacomnium turgidum* (Wahlenb.) Schwägr., *Ptilidium ciliare* (L.) Hampe, *Hylocomium splendens* (Hedw.) Bruch et al., *Tomentypnum nitens* (Hedw.) Loeske, and a number of species of the lichen genus *Cladonia* P. Browne.

Larch growth index chronology

Larch GI fluctuated periodically during the last three centuries with minimal values observed at the beginning of the nineteenth century (Fig. 4). Larch GI tended to increase after the end of the "Little Ice Age" (ca. 1850), reaching maximal values in the 1930s and 1940s. The warming onset in the 1970s led to a minor GI increase in the 1980s followed by a GI decrease until the beginning of the twenty-first century. A stronger GI increase occurred since 2008 through 2020 after the end of the "warming hiatus." The recent increases in GI values are still lower than during the 1930s and 1940s (Fig. 4).

Temporal dynamics of growth index and climate

For larch at Ary-Mas, the climate response of the GI occurred in three phases: before, after, and during the

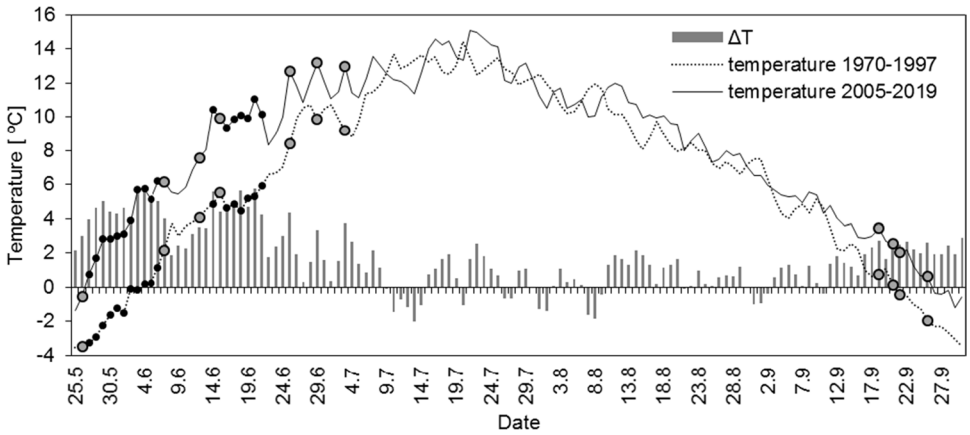

Fig. 3 Dynamics of mean daily air temperature (May–September) during the 1970–1997 and 2005–2019 periods. Bars show the difference (ΔT) in temperatures between these periods. The period with T > 0 °C increased by 8 days in spring and by 5 days in autumn. Black and gray dots mark differences at $p < 0.05$ and $p < 0.1$ significance levels, correspondingly

Table 1 Inventory data for Ary-Mas test plots

TP	Coordinates	Elevation, m a.s.l	Slope, degree	Mean DBH, cm*	Mean height, m	Mean age, y	# Stems ha^{-1}	Regeneration, stems ha^{-1}	Crown closure
1	72°27′19″N 101°57′00″E	25	2.5	16 ± 1	6.1 ± 0.4	307 ± 15	370	3000–5000	0.3
2	72°27′00″N 101°55′50″E	35	1.5	13 ± 2	5.0 ± 0.2	200 ± 16	60	4000–6000	0.1
3	72°26′23″N/101°56′06″E	60	3.0	13 ± 2	4.5 ± 0.7	143 ± 3	230	8000–10,000	0.1

*Confidence intervals indicate the standard error of the mean

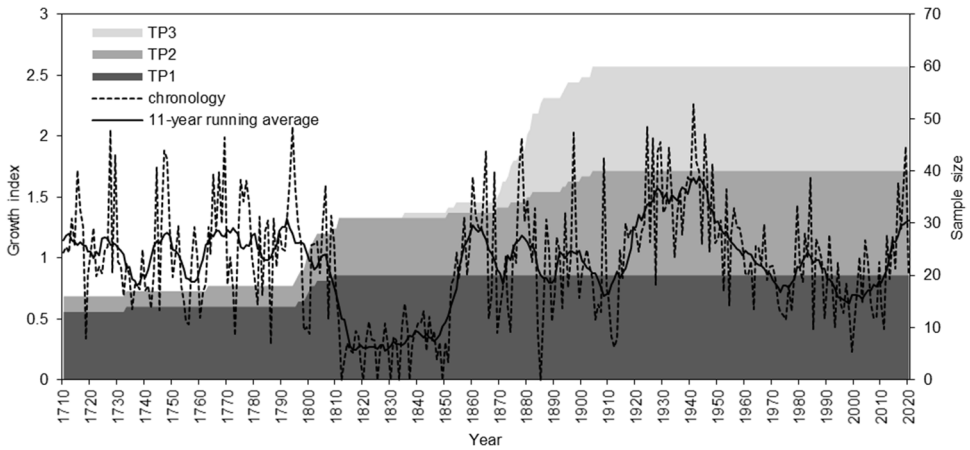

Fig. 4 Larch growth index (GI) for Ary-Mas has increased since the end of the Little Ice Age (c. 1850) and during warming in the 1930s–1940s on the test plots TP1–TP3. Warming since the 1970s led to a minor GI increase before reduced GI during the "warming hiatus" (c. 1998–2004). The number of trees represented in the chronology is indicated on the right axis

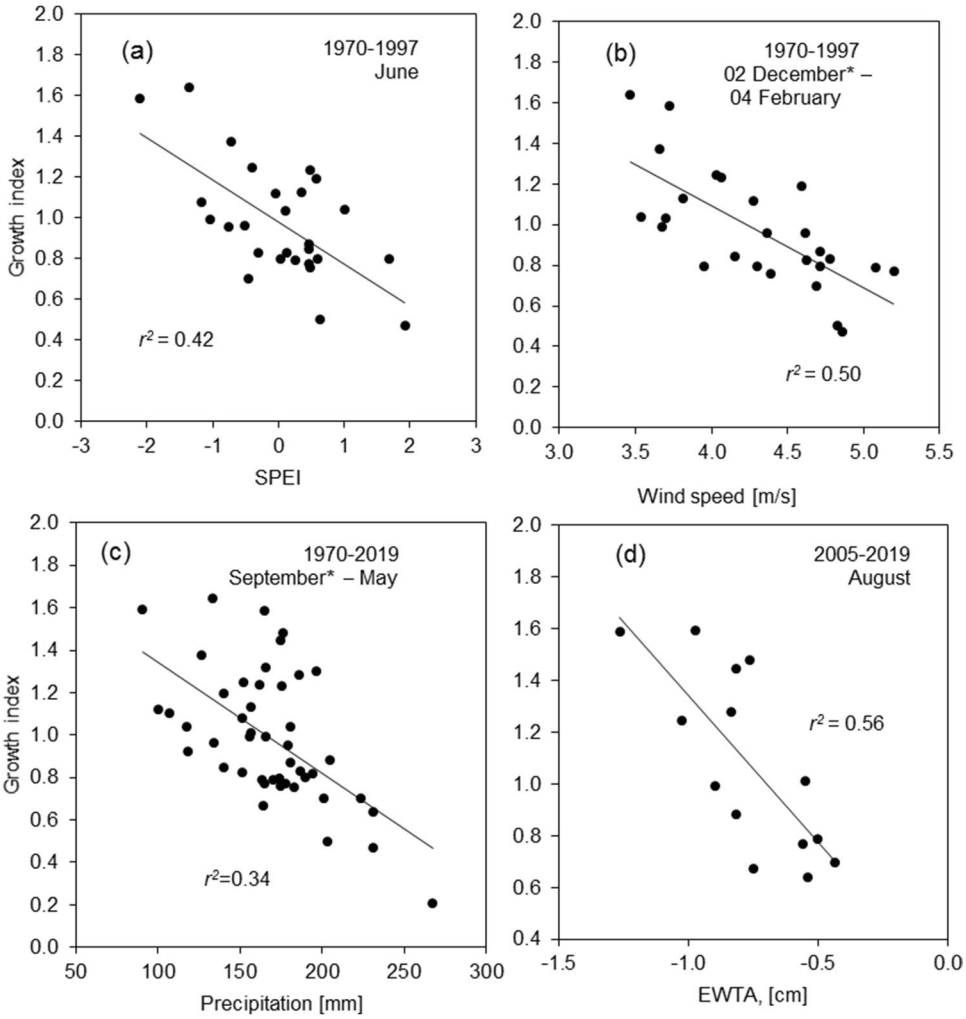

Fig. 5 Correlation of larch GI with climate variables. **a** June drought index SPEI (period 1970–1997; *N* (number of points) = 27), **b** previous December–February wind speed (period 1970–1997; *N* = 26), **c** precipitation (period 1970–2019; *N* = 47), **d** August EWTA (water storage anomalies). Period 2005–2019; *N* = 14. The symbol * denotes a month of the previous year. Trends are significant at $p < 0.05$

warming hiatus of c. 1998–2004. The first phase approximated the time interval from warming onset in the 1970s to minimal GI values in 1997 (Fig. 4). GI correlated with air temperatures at the beginning of the growth period (end of June–mid of July; Fig. 6). GI was not correlated with summer precipitation, whereas a negative correlation was observed with cold period (September–May) precipitation ($r^2 = 0.34$; Fig. 5c). The latter referred to the delay of the snow cover melt. Negative correlations were observed between GI and drought index SPEI (June) values ($r^2 = 0.42$; Fig. 5a). Significant negative correlations were observed with the winter wind's impact ($r^2 = 0.50$; Fig. 5b). The second phase coincided with the previously described "warming hiatus" period (c. 1998–2004) for which there were no significant correlations to any of the eco-climatic factors.

The third phase of the larch GI dynamics (since 2005) coincided with post-hiatus warming. We observed a significant shift between temperatures in the third (2005–2019) and first (1970–1997) phases (Fig. 6). During this phase, GI also correlated with June–July temperatures, although correlations were shifted to earlier dates (Fig. 6). A weaker (but significant) correlation appeared with autumn (06–12 September) air temperatures (Fig. 6). Larch GI was negatively correlated to EWTA (water storage anomalies) (Fig. 2d; 5d) which should be attributed to the adverse effect of "wet cold soils" on the trees' root function. Meanwhile, wind impact becomes insignificant; the latter is related to a decrease in wind speed (Fig. 2e).

Larch growth index response to climate variables: generalized linear models

Time interval 1970–1997 years

Correlation analysis identified eco-climatic variables with a significant relation to larch GI including air temperature at the beginning of the growth period, wintertime wind speed, and drought index SPEI. The dependence of larch GI on these variables is described by the following equation:

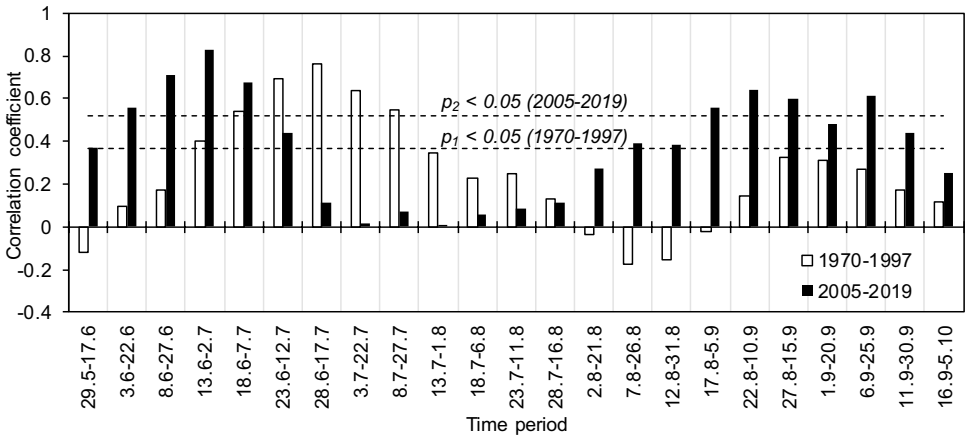

Fig. 6 Running correlations between growth index and the air temperature (window 20 days, lag 5 days). GI was significantly correlated with the temperature at the beginning and end of the growth period. In comparison with 1970–1997, correlations during the 2005–2019 period shifted to early dates in spring and to later dates in fall

$$GI = 0.49T - 0.33SPEI - 0.24V + 0.09, \quad (1)$$

where T is the air temperature (time period 25.06–19.07), *SPEI* is the June SPEI value, and V is the wintertime wind speed (02.12–04.02). Regression coefficients are significant at $p < 0.01$.

This model explained approximately 85% of the variation in GI (Fig. 7a; $R^2 = 0.85$; $p < 0.01$). Variable inputs into the intercepted dispersion were as follows: $T = 66\%$, SPEI = 5%, and $V = 11\%$. Thus, larch GI increased with increased June–July air temperature and decreased with increased winter wind speed and increased SPEI, the latter indicating decreased moisture stress.

Time interval 2005–2019

During this time interval, air temperatures at the beginning and end of the growth period and soil moisture anomalies were significant. Thus, larch GI dependence on the climate variables is described by the following equation:

$$GI = 0.462T_1 + 0.387T_2 - 0.552W - 0.016, \quad (2)$$

where T_1 and T_2 are air temperatures at the beginning (June 10–July 04) and end (September 06–12) of the annual growth period; W is the August EWTA water anomaly. Regression coefficients are significant at $p < 0.01$.

This model intercepted approximately 97% of the *GI* variability ($R^2 = 0.97$, $p < 0.01$; Fig. 7b). The contributions of the individual eco-climate variables to the model trend are: $T_1 = 58.1\%$, $T_2 = 14.5\%$, $W = 24.8\%$.

GPP and NPP trends at the Ary-Mas site and in the central Siberian Arctic

Within the Ary-Mas, larch GI strongly correlated with vegetation cover gross (GPP) and net (NPP) primary productivity (Fig. 8a, b). GPP and NPP decreasing trends were observed until the break point in 2008 with a subsequent increase (Fig. 8c). Similar increasing GPP trends were found earlier within the Kotuy site (Fig. 9; Kharuk et al. 2019).

GPP and NPP increases were observed not only within the Ary-Mas site but also throughout the central Siberian Arctic. GPP- and NPP-positive trends were observed in 14% and 22% of the territory, respectively. Negative trends covered less than 1% of the territory (Fig. 9).

Discussion

The northernmost Ary-Mas "forest island" provided a unique opportunity to investigate eco-climatic limits to tree growth. Recent increases in the radial growth of *L. gmelinii* were part of the overall increase in productivity we described for GPP and NPP, both for Ary-Mas and the overall central Siberian Arctic region. From tree recruitment patterns, we see that larch has been long-established in the "larch refugium" of TP1, a closed-canopy refugium stand in a strip of land along the Novaya River and protected from extreme wind exposure. We interpret the later recruitment dates in TP2 and TP3 as evidence that larch has migrated upslope from the refugium to form sparse stands that continue to increase in tree density (Fig. S2). Regeneration within the larch refugium was poor, while recruitment within sparse stands (3000–10,000 trees/ha) was good (e.g., Figs. S2, S3). Due to the thick moss-lichen groundcover that resists seedling root penetration, larch regeneration requires exposed mineral soil (as from cryoturbation) (Kharuk et al. 2021a; Figs. S1, S3). Seedling mostly established within wind-sheltered relief features (e.g., micro-depressions, behind the boulders or dead trees; Figs. S2, S4). A similar establishment pattern was described for shrub species

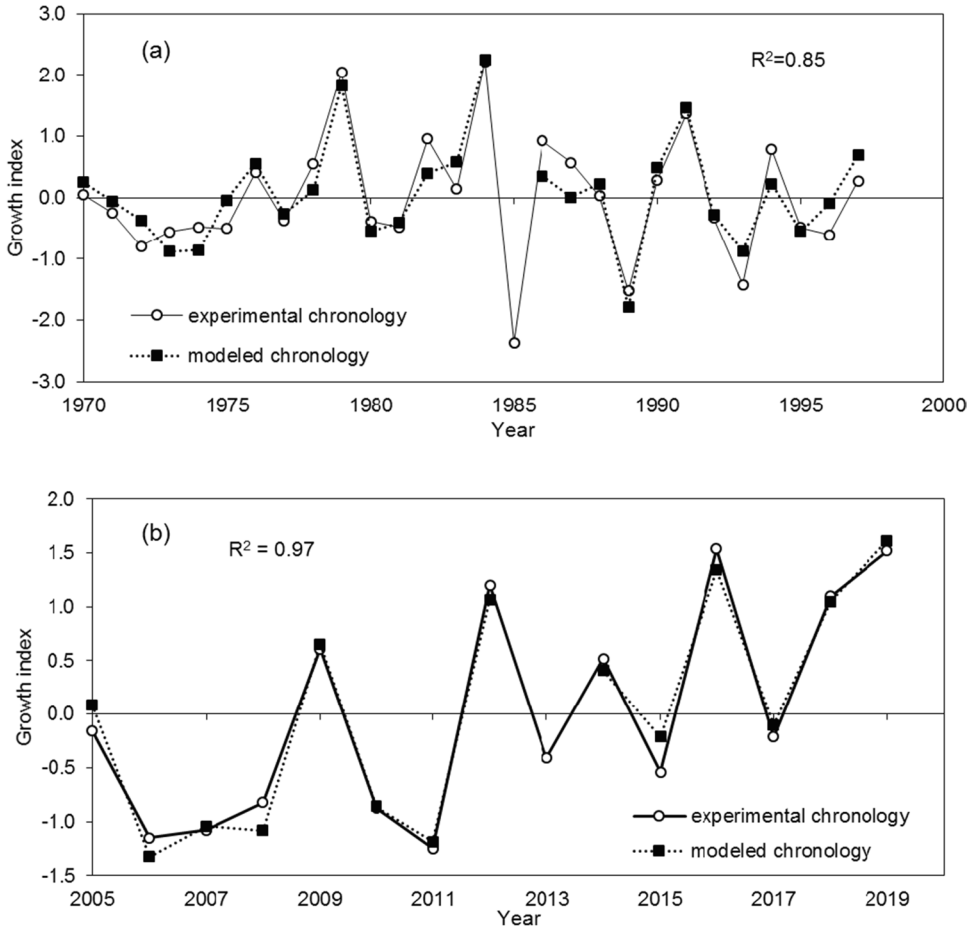

Fig. 7 Experimental and modeled growth index chronologies **a** for the 1970–1997 period and **b** for the 2005–2019 period

in North American tundra (Tape et al. 2006; Myers-Smith et al. 2019). Alongside with the harsh environment, seed availability and quality also strongly limited the advance of trees into tundra (Kharuk et al. 2013; Wieczorek et al. 2017). Regeneration was mostly observed in the vicinity of "mother trees," outside of which seedling density was low (Fig. S4). Larch also establishes new stems by layering (Fig. S5).

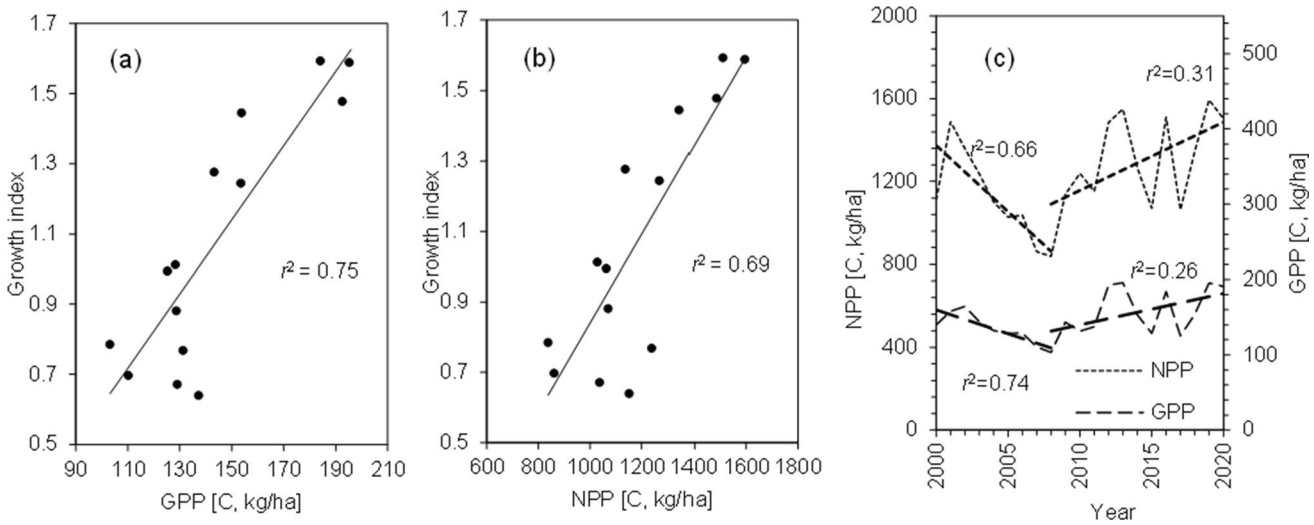

Fig. 8 **a**, **b** Correlation of larch growth index (GI) to GPP and NPP, respectively. **c** Break point regressions of GPP and NPP. GPP and NPP were averaged throughout test points TP1–TP3 (Fig. 1). Regressions are significant at $p < 0.05$

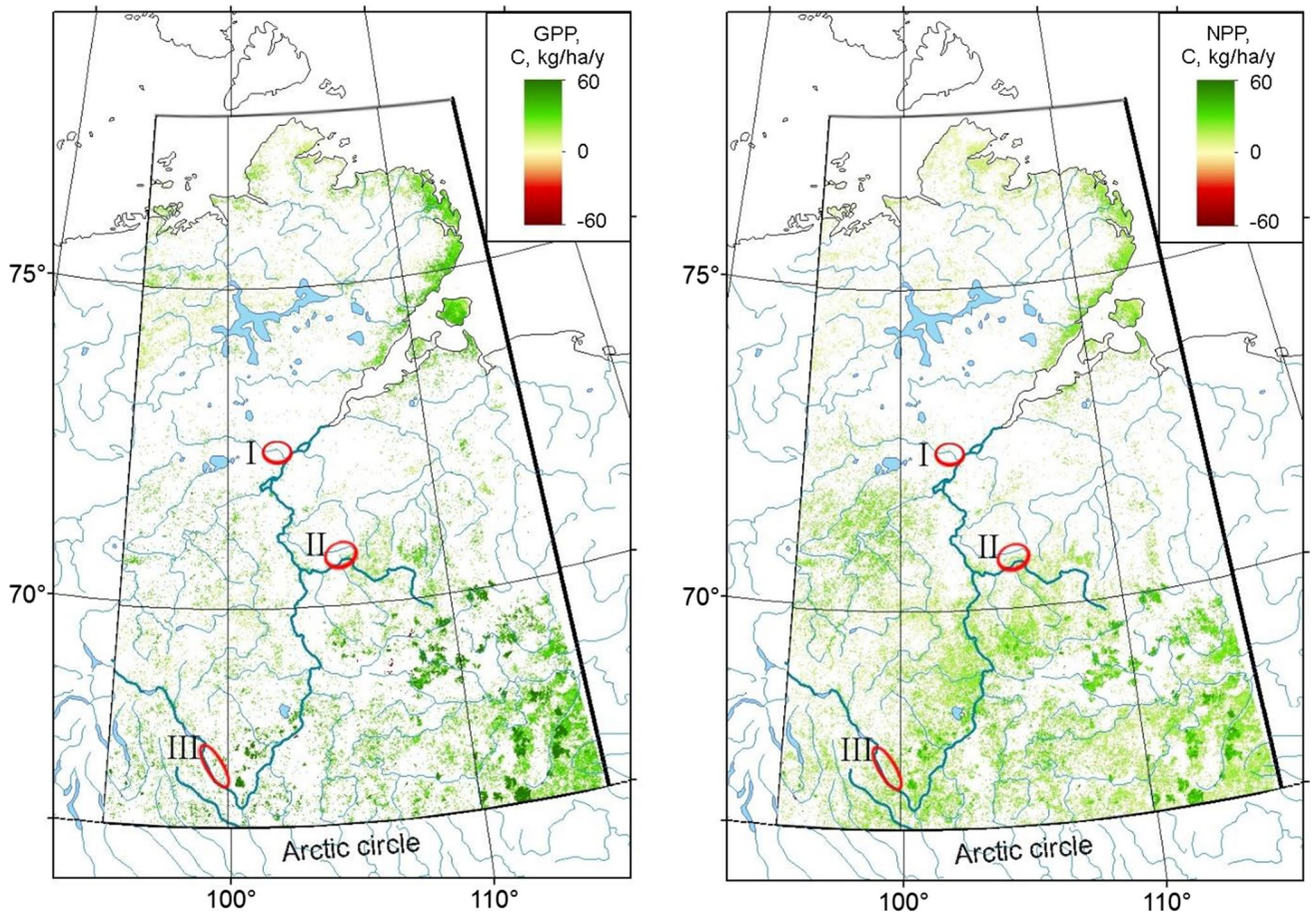

Fig. 9 Mean GPP (left) and NPP (right) trends in the central Siberian Arctic for the 2000–2020 period. Significantly increasing trends in GPP and NPP ($p < 0.05$) occurred for 14% and 22% of the territory, respectively. Negative trends in productivity were found for less than 1% of the territory The circled locations indicate the Ary-Mas location (I) and the supplementary former study sites at Kotuykan (II) and Kotuy (III) (Kharuk et al. 2013, 2019)

The response of larch GI to warming temperatures occurred in three phases. During the first phase from the 1970s to the mid-1990s, GI increased in response to warming early in the growing season and decreased in response to increased winter wind speed (Eq. (1)). The second phase from 1995 to 2005 coincided with the previously described "warming hiatus" in which GI did not vary in relation to air temperature. In both phases, an adverse winter wind's influence on larch growth was observed which was attributed to the wind-cased twig desiccation and snow abrasion, as previously described for birch at the northern treeline in the Swedish Scandes (Kullman 2005). During the third phase from 2005–2020, GI was related to air temperature both during June and during the late growing season (Eq. (2)). Temporal changes in the sensitivity of tree growth to climate has been noted in recent decades and attributed to various factors (e.g., Briffa et al. 1998; Smith et al. 1999; Lebourgeois et al. 2012). Meanwhile, since the 1970s, the wind speed has gradually decreased which led to decreased desiccation and snow abrasion effects on tree growth (Fig. 5b).

In contrast to the favorable effects of increased air temperatures, larch growth was negatively correlated to soil water content (Fig. 5d). In the permafrost zone, such so-called wet cold soils are widespread in lowlands. Low soil temperatures slow down root activity with consequent tree growth decreases. The other negative factor is a limited root oxygen supply within poorly drained soils. Note that GI also negatively correlated with "solid precipitation" (Fig. 5c), explained by the delay in snowmelt. Meanwhile, the observed decrease in soil water supported greater larch growth (Fig. 2d). In contrast, growth limitation by water availability has been described in permafrost zones (e.g., in larch habitat on mountain slopes) (Kharuk et al. 2015, 2019; Zhang et al. 2016). Larch may experience a moisture deficit at the beginning of the growth period when elevated air temperatures are sufficient for photosynthesis, while soils are still mostly frozen (Kharuk et al. 2019). In extreme cases, larches may flash needles prior to snowmelt. In summary, larch growth in Ary-Mas

was fairly well explained by the air temperatures during the growth period and soil water anomalies ($R^2 = 0.95$; Fig. 7b). The uncertainties may be related to the CO_2 fertilization effect. However, that effect is low in cold habitats (Zhu et al. 2016).

Finally, the increase in larch growth for the Ary-Mas "forest island" coincided with increased GPP and NPP, indicative of increased carbon (C) fixation in the warming Arctic climate. Similar correlations were previously reported for other larch sites within the permafrost zone (the Kotuy site, Fig. 1, and the Embenchimo site; Kharuk et al. 2015, 2019). Meanwhile, the trend for increased GPP and NPP were observed not only within these sites but also for most of the Central Siberian Arctic (Fig. 9). Those trends indicated increased C fixation by Arctic vegetation. Within the land area dominated by larch, larch is likely the one of the principal contributors to the observed increase in productivity. Even within Arctic forest-tundra where larch is a minor component, increased tree growth coincides with the "greening tundra" phenomenon (e.g., Bhatt et al. 2017). Similar observations have been reported for northern Canadian forests, where net ecosystem biomass production and black spruce growth have increased (Hember et al. 2017, 2019). In the broader view, the larch growth increase combined with positive trends of GPP and NPP suggests that the northernmost permafrost zone continues to be a carbon sink.

Conclusions

We found a complex, time-dependent relationship between larch GI and eco-climatic factors for the Ary-Mas forest. Atmospheric warming during the 1970s had only a minor effect on GI, while a strong increase in GI was associated with warming in the 2000s through 2019. Winter wind speed adversely affected larch growth from 1970 into the late 1990s followed by no significant effect during the 2005–2019 period. Larch growth was negatively impacted by cold, wet soils. Larch growth increased with decreased soil moisture in the naturally wet forest island at Ary-Mas. The temporal shifts in the response of growth to climate may be due to threshold effects of the eco-climatic factors. We expect that continued warming will support further spread of larch into the formerly treeless tundra. Our findings suggests that the northernmost permafrost larch forest remains an aboveground carbon sink.

Supplementary Information The online version contains supplementary material available at https://doi.org/10.1007/s10113-022-02016-9.

Acknowledgements Findings and conclusions are those of the authors and should not be construed to represent official U.S. government policy.

Funding The research was funded by the Tomsk State University Development Program («Priority-2030»). K.T. Smith was supported by the United States Department of Agriculture, Forest Service.

References

Abaimov AP, Zyryanova OA, Prokushkin SG (2002) Long-term investigations of larch forests in Cryolithic zone of Siberia: brief history, recent results and possible changes under global warming. Eur J For Res 5–2: 95–106. http://hdl.handle.net/2115/22155

Akaike H (1974) A new look at the statistical model identification. IEEE Trans Autom Control 19(6):716–723. https://doi.org/10.1109/TAC.1974.1100705

Allen CD, Breshears DD, McDowell NG (2015) On underestimation of global vulnerability to tree mortality and forest die-off from hotter drought in the Anthropocene. Ecosphere 6:1–55. https://doi.org/10.1890/ES15-00203.1

Andreu-Hayles L, D'Arrigo R, Anchukaitis KJ, Beck PS, Frank D, et al. (2011) Varying boreal forest response to Arctic environmental change at the Firth River Alaska. Environ Res Lett 6:041004. https://doi.org/10.1088/1748-9326/6/4/049502

Annals of the State Reserve "Taimyrsky" (n.d.) http://taimyrsky.ru/letopis/letopis.htm

Bhatt US, Walker DA, Raynolds MK, Bieniek PA, Epstein HE et al (2017) Changing seasonality of panarctic tundra vegetation in relationship to climatic variables. Environ Res Lett 12(5):055003. https://doi.org/10.1088/1748-9326/aa6b0b

Bondarev A (1997) Age distribution patterns in open boreal Dahurican larch forests of Central Siberia. For Ecol Manag 93:205–214. https://doi.org/10.1016/S0378-1127(96)03952-7

Briffa KR, Schweingruber FH, Jones PD (1998) Trees tell of past climates: but are they speaking less clearly today? Philos Trans R Soc Lond B 353:65–73. https://doi.org/10.1098/rstb.1998.0191

Conover WJ (1999) Practical nonparametric statistics, Wiley series in probability and mathematical statistics: applied probability and statistics. Wiley, 608 pp

Cook ER, Holmes RL (1986) User's manual for program ARSTAN. In: Holmes RL, Adams RK, Fritts HC (ed) Tree-ring chronologies of Western North America: California, Eastern Oregon and Northern Great Basin, Chronology Series 6, Laboratory of Tree-Ring Research, Tucson, pp 50–65

Esper J, Frank DC, Büntgen U, Verstege A, Hantemirov RM, et al. (2010) Trends and uncertainties in Siberian indicators of 20th century warming. Glob Change Biol 16:386–398. https://doi.org/10.1111/j.1365-2486.2009.01913.x

Fakhrutdinova VV, Benkova VE, Shashkin AV (2017) Climatic signals in tree ring anatomical structure of *Larix gmelinii* growing under contrasting hydrothermal conditions within the forest-tundra ecotone. Biol Bull Russ Acad Sci 44:634–642. https://doi.org/10.1134/S1062359017050089

Fernandes R, Leblanc SG (2005) Parametric (modified least squares) and non-parametric (Theil–Sen) linear regressions for predicting biophysical parameters in the presence of measurement errors. Remote Sens Environ 95(3):303–316. https://doi.org/10.1016/j.rse.2005.01.005

Gulev SK, Thorne PW, Ahn J, Dentener FJ, Domingues CM et al (2021) Changing state of the climate system. In: Climate Change 2021: the physical science basis. Contribution of Working Group I to the Sixth Assessment Report of the Intergovernmental Panel on Climate Change. Cambridge University Press. In Press. https://www.ipcc.ch/report/ar6/wg1/downloads/report/IPCC_AR6_WGI_Full_Report.pdf

Harsch M, Hulme P, McGlone M, Duncan R (2009) Are treelines advancing? A global meta-analysis of treeline response to climate warming. Ecol Lett 12:1040–1049. https://doi.org/10.1111/j.1461-0248.2009.01355.x

Hember RA, Kurz WA, Coops NC (2017) Increasing net ecosystem biomass production of Canada's boreal and temperate forests despite decline in dry climates. Glob Biogeochem Cycles 31:134–158. https://doi.org/10.1002/2016GB005459

Hember RA, Kurz WA, Girardin MP (2019) Tree ring reconstructions of stemwood biomass indicate increases in the growth rate of black spruce trees across boreal forests of Canada. J Geophys Res Biogeosci 124:2460–2480. https://doi.org/10.1029/2018JG004573

Holmes RL (1983) Computer-assisted quality control in tree-ring dating and measurement. Tree-Ring Bulletin 44: 69–75

IBM SPSS Statistics Base V27. IBM Corp. 220 p. Available at: https://www.ibm.com/docs/en/SSLVMB_27.0.0/pdf/en/IBM_SPSS_Statistics_Base.pdf

Kharuk VI, Dvinskaya ML, Ranson KJ, Im ST (2005) Expansion of evergreen conifers to the larch-dominated zone and climatic trends. Russ J Ecol 36:164–170. https://doi.org/10.1007/s11184-005-0055-5

Kharuk VI, Ranson KJ, Im ST, Dvinskaya ML (2006) Forest-tundra larch forests and climatic tends. Russ J Ecol 37(5):291–298. https://doi.org/10.1134/S1067413606050018

Kharuk VI, Ranson KJ, Im ST, Oskorbin PA, Dvinskaya ML, et al. (2013) Tree line structure and dynamics at the northern limit of the larch forest: Anabar Plateau, Siberia Russia. Arct Antarct Alp 45(4):526–537. https://doi.org/10.1657/1938-4246-45.4.526

Kharuk VI, Ranson KJ, Im ST, Petrov IA (2015) Climate-induced larch growth response within Central Siberian permafrost zone. Environ Res Lett 10:125009. https://doi.org/10.1088/1748-9326/10/12/125009

Kharuk VI, Im ST, Petrov IA, Dvinskaya ML, Fedotova EV, et al. (2017) Fir decline and mortality in the southern Siberian mountains. Reg Environ Change 17(3):803–812. https://doi.org/10.1007/s10113-016-1073-5

Kharuk VI, Ranson KJ, Petrov IA, Dvinskaya ML, Im ST, et al. (2019) Larch (*Larix dahurica* Turcz) growth response to climate change in the Siberian permafrost zone. Reg Environ Change 19:233–243. https://doi.org/10.1007/s10113-018-1401-z

Kharuk VI, Ponomarev EI, Ivanova GA, Dvinskaya ML, Coogan SCP et al (2021) Wildfires in the Siberian taiga. Ambio 50:1953–1974. https://doi.org/10.1007/s13280-020-01490-x

Kharuk VI, Im ST, Petrov IA, Dvinskaya ML, Shushpanov AS, et al. (2021) Climate-driven conifer mortality in Siberia. Glob Ecol Biogeogr 00:1–14. https://doi.org/10.1111/geb.13243

Kirdyanov AV, Prokushkin AS, Tabakova MA (2013) Tree-ring growth of Gmelin larch under contrasting local conditions in the north of Central Siberia. Dendrochronologia 31(2):114–119. https://doi.org/10.1016/j.dendro.2012.10.003

Kullman L (2005) Wind-conditioned 20th century decline of birch treeline vegetation in the Swedish Scandes. Arctic 58(3):286–294. https://doi.org/10.1016/j.dendro.2012.10.003

Kullman L, Kjallgren L (2006) Holocene pine tree-line evolution in the Swedish Scandes: recent tree-line rise and climate change in a long-term perspective. Boreas 35:159–168. https://doi.org/10.1111/j.1502-3885.2006.tb01119.x

Landerer F (2019) JPL TELLUS GRACE Level-3 Monthly LAND Water-Equivalent-Thickness Surface-Mass Anomaly Release 6.0 in netCDF/ASCII/GeoTIFF Formats. Ver. 6.0. PO.DAAC, CA, USA. Dataset accessed [2022-09-22] at doi: https://doi.org/10.5067/TELND-3AJ06

Lebourgeois F, Merian P, Courdier F, Ladier J, Dreyfus P (2012) Instability of climate signal in tree-ring width in Mediterranean mountains: a multi-species analysis. Trees 26:715–729. https://doi.org/10.1007/s00468-011-0638-7

Lu X, Liang E, Wang Y, Babst F, Camarero JJ (2021) Mountain treelines climb slowly despite rapid climate warming. Glob Ecol Biogeogr 30:305–315. https://doi.org/10.1111/geb.13214

McMahon SM, Parker GG, Miller DR (2010) Evidence for a recent increase in forest growth. Proc Natl Acad Sci 107:3611–3615. https://doi.org/10.1073/pnas.0912376107

Myers-Smith IH, Thomas HJD, Bjorkman AD (2019) Plant traits inform predictions of tundra responses to global change. New Phytol 221:1742–1748. https://doi.org/10.1111/nph.15592

Norina BN (1978) Ary-Mas. Enviromental conditions, flora and vegetation of the northernmost forest massif in the world. Leningrad: Nauka. 190 pp. (In Russian) http://byrranga.ru/docs/015.pdf

Running SW, Zhao M (2015) Daily GPP and annual NPP (MOD17A2/A3) products NASA Earth Observing System MODIS Land Algorithm. Useŕs Guide. Version 3.0 For Collection 6

Running SW, Zhao M (2019) User's guide daily GPP and annual NPP (MOD17A2H/A3H) and year-end gap-filled (MOD17A2HGF/A3HGF) products NASA Earth Observing System MODIS Land Algorithm (For Collection 6), Version 4.2, June 10th, 2019

Ryan SE, Porth LS (2007) A tutorial on the piecewise regression approach applied to bedload transport data. Gen. Tech. Rep. RMRS-GTR-189. Fort Collins, CO: U.S. Department of Agriculture, Forest Service, Rocky Mountain Research Station. 41 p

Sen PK (1968) Estimates of the regression coefficient based on Kendall's tau. J Am Stat Assoc 63(324):1379–1389. https://doi.org/10.1080/01621459.1968.10480934

Shiyatov SG, Terent'ev MM, Fomin VV, Zimmermann NE (2007) Altitudinal and horizontal shifts of the upper boundaries of open and closed forests in the Polar Urals in the 20th century. Russ J Ecol 38: 223–227. https://doi.org/10.1134/S1067413607040017

Smith KT, Čufar K, Levanic T (1999) Temporal stability and dendroclimatology in silver fir and red spruce. Phyton 39:117–122

Tabachnick BG, Fidell LS (2013) Using multivariate statistics (6th ed). Boston, MA: Pearson. 1072 p

Tape K, Sturm M, Racine C (2006) The evidence for shrub expansion in Northern Alaska and the Pan-Arctic. Glob Chang Biol 12(4):686–702. https://doi.org/10.1111/j.1365-2486.2006.01128.x

The Forest fund of Russia (as for 1st January 2003). Reference book. Moscow: VNIILM, 2003. 640 pp. (In Russian)

Vicente-Serrano SM, Beguería S, López-Moreno JI (2010) A multiscalar drought index sensitive to global warming: the standardized precipitation evapotranspiration index. J Clim 23:1696–718. https://doi.org/10.1175/2009JCLI2909.1

Vickers H, Hogda KA, Solbo S, Karlsen SR, Tommervik H, et al. (2016) Changes in greening in the high arctic: insights from a 30-year AVHRR max NDVI dataset for Svalbard. Environ Res Lett 11(10):105004. https://doi.org/10.1088/1748-9326/11/10/105004

Wieczorek M, Kruse S, Epp LS, Kolmogorov A, Nikolaev AN et al (2017) Dissimilar responses of larch stands in northern Siberia to increasing temperatures—a field and simulation based study. Ecology 98(9):2343–2355. https://doi.org/10.1002/ecy.1887

Zhang X, Ba X, Chang Y, Chen Z (2016) Increased sensitivity of Dahurian larch radial growth to summer temperature with the rapid warming in Northeast China. Trees 30:1799–1806. https://doi.org/10.1007/s00468-016-1413-6

Zhu Z, Piao S, Myneni R, Huang M, Zeng Z et al (2016) Greening of the Earth and its drivers. Nat Clim Chang 6: 791–795. https://doi.org/10.1038/nclimate3004

Supplementary

Fig. S1. Larch seedling established mostly within patches of bare soil at Ary-Mas (Site I in Fig. 1).

Fig. S2. In the windy habitat, larch seedling establishment relied on wind shelters within microtopographic features (e.g., dead trees from the former epoch, boulders, local depressions) at Kotuy (Site II on the Fig. 1).

Fig. S3. Within the refugium, regeneration density is low due to the thick “moss pillow”.

Fig. S4. Majority of regeneration occurred in the vicinity of a “mother larch” having survived the Little Ace Age (Site II on the Fig. 1).

Fig. S5. Larch clusters which originated due to vegetative layering (Site II on the Fig. 1).